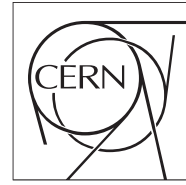


The Compact Muon Solenoid Experiment
Analysis Note



The content of this note is intended for CMS internal use and distribution only

27 October 2010

Opposite sign di-lepton SUSY search at $\sqrt{s} = 7$ TeV in 2011 data

M. Edelhoff, L. Feld, N. Mohr, D. Sprenger

I. Physikalisches Institut B, RWTH Aachen University, Germany

Abstract

We present a search for Supersymmetry in opposite sign di-lepton final states using the data from 2011 proton-proton-running of the Large Hadron Collider. The final state signature consists of leptons, several hard jets and missing transverse energy. Since we observe good agreement of data to simulation and our background prediction methods, we conclude that there is no sign of flavour correlated di-lepton production accompanied by high jet activity and large missing transverse energy in the dataset of 204 pb^{-1} . We report an upper limit on the flavour correlated production of a new physics model within acceptance of our event selection.

Preliminary version

Contents

17	1 Disclaimer	3
18	2 Introduction	3
19	3 Signal	3
20	4 Physics objects	4
21	4.1 PAT workflow	4
22	4.2 Datasets	4
23	4.3 Simulated datasets	4
24	4.4 Common event selection	6
25	4.5 Muons	6
26	4.6 Electrons	6
27	4.7 Light lepton isolation	6
28	4.8 Taus	7
29	4.9 Jets and missing transverse energy	7
30	4.10 Trigger	7
31	4.10.1 Lepton trigger selection	8
32	4.10.2 Lepton H_T cross trigger trigger selection	8
33	4.10.3 Tau trigger selection	9
34	5 Efficiency for electrons and muons	9
35	6 Event selection	9
36	6.1 Preselection	10
37	6.2 Definition of the signal regions	10
38	6.2.1 2010 signal region	11
39	6.2.2 High H_T signal region	11
40	6.2.3 High \cancel{E}_T signal region	12
41	7 Background prediction methods	13
42	7.1 Different flavour subtraction	13
43	7.2 Z boson prediction	14
44	7.3 Preselection region	15
45	8 Results	15
46	9 Limit	16
47	10 Conclusion	17

1 Disclaimer

Please note that most of the methods used in this analysis have also been documented in SUS-08-004, SUS-09-002 (AN-2009/83), AN-2010/167 and AN-2010/373.

2 Introduction

The standard model of particle physics (SM) leads to a number of unsolved issues like the hierarchy problem and it provides no solution for pressing questions arising from astrophysical observations, most notably dark matter. In Supersymmetry (SUSY) a natural candidate for dark matter can be found if R-parity conservation is assumed. Supersymmetric particles (sparticles) have not been observed up to now which implies that they have to be heavy. On the other hand to provide a solution to the hierarchy problem their masses have to be in the TeV range. These prejudices lead to a signature of (many) hard jets and large missing transverse energy.

Of special interest are robust signatures in leptonic final states which can be probed with the CMS experiment. If R-parity is conserved the lightest neutralino escapes detection and no mass peaks can be observed in SUSY decay chains. A key point after discovery will be the determination of the sparticle properties.

The purpose of this analysis is to observe or exclude a significant excess of di-leptons over the various backgrounds. The dataset consists of 204 pb^{-1} of proton-proton collisions collected by CMS during LHC running in 2011.

In Sec. 3 we define the signal benchmark points, that are used in this analysis. Section 4 describes the technical details of the object selection and in Sec. 5 we discuss lepton efficiencies used in the background prediction. Section ?? describes a method to determine the contribution of non-prompt leptons in the final event selection. In Sec. we define the signal regions, including a discussion of the main Standard Model backgrounds and their yields. Section 7.1 deals with the background prediction methods, which are used to predict the number of Standard Model backgrounds in the signal regions. The results are presented in Sec. 8. Finally we set a limit and conclude.

3 Signal

The CMS minimal supergravity low-mass benchmark points have been designed to cover different decay modes of the neutralinos within supersymmetry. The mass spectra of the benchmark points have been calculated using the Softsusy code [1]. All branching ratios have been calculated with the SUSYHit program [2] and the events are simulated using Pythia [3]. The k-factor for the cross section at 7 TeV is calculated using a modified version of Prospino 2 [4]. In mSUGRA observable signal is produced strongly followed by (very) long decay chains leading to several hard jets (at least two). The escaping neutralino leads to missing transverse energy. This fact allows to define a search region to observe an excess over the SM and is used as main event selection as described in Section 6. It consists of

- Two opposite sign same flavour leptons within acceptance of $p_T > 10 \text{ GeV}$ ¹⁾ and $|\eta| < 2.4$.
- High $H_T > 350 \text{ GeV}$ with at least two jets to be as model independent as possible.
- High $\cancel{E}_T > 150 \text{ GeV}$, which is set as such that we expect roughly one di-leptonic $t\bar{t}$ event in this years dataset.

The number of expected events in a given di-lepton channel varies with the mSUGRA point realised by nature. A range of benchmark points has been studied to anticipate different possible signal constellations and not tune towards a specific set of parameters. Figure ?? shows the fraction of di-leptonic events splitted by flavour for a di-lepton selection on generator level. In all studied benchmark points the flavour correlated production dominates over the uncorrelated production.

¹⁾ In the first version of the note the lepton p_T cut was at 5 GeV, which gives a better sensitivity to low mass mSUGRA. The electrons are not fully commissioned to 5 GeV and since there was no excess observed, we took a conservative approach to raise the threshold for this year and to continue commissioning the electron identification at low p_T , such that we can use low p_T thresholds in the next year.

4 Physics objects

4.1 PAT workflow

From the AOD samples so called Pat-Tuples have been created using the following tags of the Physics Analysis Toolkit (PAT) in CMSSW_4_2_X.

```
cmsrel CMSSW_4_2_3
cd CMSSW_4_2_3/src
cmsenv
addpkg PhysicsTools/PatAlgos V08-06-25
addpkg PhysicsTools/PatExamples V00-05-17

# deterministic calculation of FastJet corrections
addpkg RecoJets/Configuration V02-04-16
addpkg RecoJets/JetAlgorithms V04-01-00
addpkg RecoJets/JetProducers V05-05-03

addpkg MuonAnalysis/MuonAssociators V01-13-00
addpkg PhysicsTools/Configuration V00-10-14

addpkg RecoTauTag/RecoTau RecoTauDAVerticesPatch_V5
addpkg RecoTauTag/TauTagTools RecoTauDAVerticesPatch_V5
addpkg RecoTauTag/Configuration RecoTauDAVerticesPatch_V5

cvs co -d__temp__ -r1.1 UserCode/SuSyAachen/Configuration/python/pfTools.py
/bin/mv __temp__/pfTools.py PhysicsTools/PatAlgos/python/tools
rm -r __temp__

cvs co -rV00-04-48 -dSuSyAachen UserCode/SuSyAachen
```

All physics objects necessary for this analysis are included in the Pat-Tuples.

4.2 Datasets

We perform the analysis on events triggered by leptonic, hadronic and cross-object triggers and therefore use several primary datasets reconstructed in CMSSW_4_2_X. All datasets used are listed in Tab. 1.

Table 1: Datasets used in this analysis.

DBS datasetpath
/DoubleElectron/Run2011A-May10ReReco-v1/AOD
/DoubleElectron/Run2011A-PromptReco-v4/AOD
/DoubleMu/Run2011A-May10ReReco-v1/AOD
/DoubleMu/Run2011A-PromptReco-v4/AOD
/MuEG/Run2011A-May10ReReco-v1/AOD
/MuEG/Run2011A-PromptReco-v4/AOD
/ElectronHad/Run2011A-May10ReReco-v1/AOD
/ElectronHad/Run2011A-PromptReco-v4/AOD
/MuHad/Run2011A-May10ReReco-v1/AOD
/MuHad/Run2011A-PromptReco-v4/AOD
/HT/Run2011A-May10ReReco-v1/AOD
/HT/Run2011A-PromptReco-v4/AOD

We select only events that enter the officially produced good-run-list

```
/afs/cern.ch/cms/CAF/CMSCOMM/COMM_DQM/certification/Collisions11/7TeV/Reprocessing/
```

123 Cert_160404-163869_7TeV_May10ReReco_Collisions11_JSON.txt

and the total integrated luminosity amounts to

$$\mathcal{L}_{int} = (204 \pm 8) \text{ pb}^{-1}. \quad (1)$$

124 4.3 Simulated datasets

125 All simulated samples from CMSSW_4_2_X are listed in Tab 2. Please note that for the final version the proper
126 Madgraph samples will be used (as soon as they are available).

Table 2: Used CMSSW datasets from 4.2_X.

DBS datasetpath	No. events	σ_{LO} [pb]	Name
/LMX_SUSY_sftsht_7TeV-pythia6/Fall10-START38_V12-v1/AODSIM	200000	varies	SUSY LMX
/TTJets_TuneZ2_7TeV-madgraph-tauola/Fall10-START38_V12-v2/AODSIM	1443404	90	tt+jets
/DYJetsToLL_TuneZ2_M-50_7TeV-madgraph-tauola/Fall10-START38_V12-v2/AODSIM	1084921	2350	Z+jets
/WToENu_TuneZ2_7TeV-pythia6/Fall10-START38_V12-v1/AODSIM	189069	8057	W+jets
/WToMuNu_TuneZ2_7TeV-pythia6/Fall10-START38_V12-v1/AODSIM	189069	8057	W+jets
/WToTauNu_TuneZ2_7TeV-pythia6/Fall10-START38_V12-v1/AODSIM	189069	8057	W+jets
/QCD_TuneD6T_HT-100To250_7TeV-madgraph/Fall10-START38_V12-v1/AODSIM	10842371	7000000	QCD
/QCD_TuneD6T_HT-250To500_7TeV-madgraph/Fall10-START38_V12-v1/AODSIM	4873036	171000	QCD
/QCD_TuneD6T_HT-500To1000_7TeV-madgraph/Fall10-START38_V12-v1/AODSIM	4034762	520	QCD
/QCD_TuneD6T_HT-1000ToInf_7TeV-madgraph/Fall10-START38_V12-v1/AODSIM	1541261	83	QCD

127 Each dataset is scaled to the desired luminosity if not illustrated differently. Additionally a k-factor has been
128 applied for some of the datasets. The MC is reweighted to correct for the difference in the vertex multiplicity
129 distribution as described in [25].

130 4.4 Common event selection

131 To select good collision events we require the event to contain a good primary vertex, which has to pass the
132 following conditions

```
133 !isFake
134 ndof > 4
135 abs(z) <= 24
136 position.Rho <= 2.
```

137 4.5 Muons

138 The acceptance of the muons is restricted to $p_T > 5 \text{ GeV}$ and $|\eta| < 2.4$. Each muon has to be identified as a global
139 muon and tracker muon. The track of the muon in the inner tracker has to have at least 11 hits and a χ^2/ndf of
140 the global muon track below 10. The impact parameter of the muon track with respect to the position of the first
141 deterministic annealing (DA) vertex is required to be below $200 \mu\text{m}$ in x - y and within 1 cm in z . Additionally we
142 require the muons to be well measured by the request that the relative error from the track-fit is below 10%. The
143 combined energy sum in cone of size $dR = 0.3$ around each muon has to be smaller than 15% of its energy. All cuts
144 are summarised in Table 3.

145 4.6 Electrons

146 The acceptance of the electrons is restricted to $p_T > 10 \text{ GeV}$ and $|\eta| < 2.5$. We restrict ourselves to the ECALs
147 fiducial volume, thus exclude electrons within $1.4442 < \eta < 1.566$.

148 Additionally, a conversion rejection is performed requiring that the electron track has maximally one lost hit in
149 the tracker. We remove electrons from conversions via partner track finding, i.e. if there is a general track within

Table 3: Overview of the muon selection.

Name	Pat memberfunction	Cut
p_T	pt()	$\geq 5.$
$ \eta $	abs(eta())	≤ 2.4
GlobalPromptTight	muonID('GlobalMuonPromptTight')	
TrackerMuon	isTrackerMuon()	
Number of hits	track.numberOfValidHits	≥ 11
Good track fit	track.ptError()/track.pt()	≤ 0.1
Impact parameter	abs(dxy(pv))	≤ 0.02
Impact parameter	abs(dz(pv))	≤ 1
Isolation	(isolationR03().hadEt + isolationR03().emEt + isolationR03().sumPt) / pt	≤ 0.15

150 $Dist < 0.02$ cm and $\Delta \cot \theta < 0.02$ [?]. The impact parameter of the electron track with respect to the position
 151 of the primary DA vertex position is required to be below $400 \mu\text{m}$ in x - y and smaller than 1 cm in z . The cuts are
 152 summarised in Table 4.

Table 4: Overview of the electron selection.

Name	Pat memberfunction	Cut
p_T	pt()	$\geq 5.$
$ \eta $	abs(eta())	≤ 2.4
Identification	WP95	
Lost hits	gsfTrack->trackerExpectedHitsInner().numberOfHits()	≤ 1
Partner track finding	!(Dist and $\Delta \cot \theta$)	≤ 0.02
Impact parameter	abs(dxy(pv))	≤ 0.04
Impact parameter	abs(dz(pv))	≤ 1
Isolation Barrel	(dr03HcalTowerSumEt + max(0., dr03EcalRecHitSumEt-1.) + dr03TkSumPt) / pt	≤ 0.15
Isolation Barrel	(dr03HcalTowerSumEt + dr03EcalRecHitSumEt + dr03TkSumPt) / pt	≤ 0.15

153 4.7 Light lepton isolation

A combined relative lepton isolation has been used. The isolation uses information from both calorimeters and the silicon tracker. The isolation value (I_{so}) is given by the ratio of the sum of all p_T objects within a cone in η - ϕ -space of $\Delta R = \sqrt{\Delta\eta^2 + \Delta\phi^2} < 0.4$ around the lepton and the lepton p_T . It has been pre-calculated in PAT using

$$I_{so} = \frac{\left[\sum_{photons} p_T + \sum_{neutral\ hadrons} p_T + \sum_{charged\ hadrons} p_T \right]_{dR < 0.4}}{p_T} \quad (2)$$

154 where the first sum runs over the transverse momentum of all particle flow photons, the second sum runs over the
 155 transverse momentum of all neutral hadrons and the third sum runs over the transverse momentum deposited as
 156 charged hadrons within the cone.

157 The isolation for prompt muons obtained from the sPlot technique (Sec.??) is shown Figure ?? and the cut value is
 158 chosen to be $I_{so} < 0.2$. The distribution for electrons is displayed in Figure ?? and the cut is placed at $I_{so} < 0.2$
 159 to obtain a similar rejection and efficiency for electrons and muons. The background shapes evaluated from data
 160 are discussed in Sec. ??.

161 4.8 Taus

162 **TODO:** Matthias tau selection

4.9 Jets and missing transverse energy

The anti-kt jet algorithm [6] with a cone size of 0.5 in ΔR is used. Jets are clustered from all reconstructed particle flow particles. We remove jets that are within $\Delta R < 0.4$ to a lepton passing our full lepton selection. Thus we obtain fully lepton cleaned jets in our final selection. The jets are corrected up to level 3 using MC jet energy corrections [17] from the Summer11 (GlobalTag: GR_R_42_V12, START42_V12) production. To correct for PileUp the L1FastJet subtraction using the latest JetMET prescription is applied.

Each corrected jet is required to have a p_T above 30 GeV and the jet axis has to be within $|\eta| < 3$. This relatively tight η cut is used to be able to include tracker information in the jet identification for a large part of the η acceptance and not to rely on the hadronic calorimeter only. Thus, one is able to fully profit from the particle flow algorithm. Each jet has to pass the "FIRSTDATA" "LOOSE" Particle Flow Jet ID criteria, which are used to suppress fake, noise, and badly reconstructed jets, while still retaining as much real jets as possible [18].

The missing transverse energy (MET) is based on the sum of all particle momenta reconstructed using the particle flow event reconstruction (pfMET).

4.10 Trigger

We collect events using three different trigger streams:

- (20,10) GeV ee , $e\mu$, $\mu\mu$ events are selected using the lepton trigger selection.
- (10,10), (10,5), (5,5) GeV ee , $e\mu$, $\mu\mu$ events are selected using the lepton H_T cross object trigger selection.
- (5,15), (10,15), (15,15) GeV $\mu\tau$, $e\tau$, $\tau\tau$ events are selected using the tau trigger selection.

4.10.1 Lepton trigger selection

To collect events for the (20,10) GeV di-lepton selection we use an OR of the following double lepton high level trigger (HLT) paths

- HLT_Ele17_CaloIdL_CaloIsoVL_Ele8_CaloIdL_CaloIsoVL_v*
- HLT_Ele17_CaloIdT_TrkIdVL_CaloIsoVL_TrkIsoVL_Ele8_CaloIdT_TrkIdVL_CaloIsoVL_TrkIsoVL_v*
- HLT_Mu8_Ele17_CaloIdL_v*
- HLT_Mu17_Ele8_CaloIdL_v*
- HLT_Mu10_Ele10_CaloIdL_v*
- HLT_DoubleMu6*
- HLT_DoubleMu7_v*
- HLT_Mu13_Mu7_v*

We check that the prescale of each trigger is set to one for all run ranges.

We measure the efficiency in an orthogonal event selection using events triggered by purely hadronic triggers.

Table 5: Double lepton high level trigger efficiencies.

HLT path	Thresh. [GeV]	Pathname	ϵ
H_T	100	HLT_HT100U	$99.8 \pm 0.1\%$
H_T	140	HLT_HT140U	$99.7 \pm 0.1\%$
H_T	150	HLT_HT150U	$99.7 \pm 0.1\%$

The measured efficiencies are listed in Table 5. We obtain an efficiency of $(99.7 \pm 0.1)\%$, $((99.7 \pm 0.1)\%$, $(99.7 \pm 0.1)\%$ for the ee ($e\mu$, $\mu\mu$) trigger with respect to the final di-lepton selection, respectively.

4.10.2 Lepton H_T cross trigger trigger selection

To collect events for low lepton p_T range (e 10, μ 5) GeV di-lepton plus H_T cross-object triggers are used. We use an OR of the following double lepton H_T HLT paths

- HLT_DoubleEle8_CaloIdL_TrkIdVL_HT160_v*
- HLT_DoubleEle8_CaloIdL_TrkIdVL_HT150_v*
- HLT_DoubleMu3_HT160_v*
- HLT_DoubleMu3_HT150_v*
- HLT_Mu3_Ele8_CaloIdL_TrkIdVL_HT160_v*
- HLT_Mu3_Ele8_CaloIdL_TrkIdVL_HT150_v*

We check that the prescale of each trigger is set to one for all run ranges.

We measure the leptonic efficiency in event selection using events triggered by purely hadronic (H_T) triggers, while the hadronic efficiency is measured using events collected by di-lepton triggers. We assume no correlation between the hadronic and leptonic part of the trigger and give the total efficiency as a product of both.

Table 6: Double lepton H_T cross object trigger high level trigger efficiencies.

HLT path	Thresh. [GeV]	Pathname	ϵ
H_T	100	HLT_HT100U	$99.8 \pm 0.1\%$
H_T	140	HLT_HT140U	$99.7 \pm 0.1\%$
H_T	150	HLT_HT150U	$99.7 \pm 0.1\%$

The measured efficiencies are listed in Table 6. We obtain an efficiency of $(99.7 \pm 0.1)\%$, $((99.7 \pm 0.1)\%$, $(99.7 \pm 0.1)\%$ for the ee ($e\mu$, $\mu\mu$) trigger with respect to the final di-lepton selection, respectively.

4.10.3 Tau trigger selection

To collect event including taus in the final state we use an OR of the following double lepton high level trigger (HLT) paths

- **TODO**tau trigger selection

We check that the prescale of each trigger is set to one for all run ranges.

We measure the efficiency in an orthogonal event selection using events triggered by purely hadronic triggers.

Table 7: Tau high level trigger efficiencies.

HLT path	Thresh. [GeV]	Pathname	ϵ
H_T	100	HLT_HT100U	$99.8 \pm 0.1\%$
H_T	140	HLT_HT140U	$99.7 \pm 0.1\%$
H_T	150	HLT_HT150U	$99.7 \pm 0.1\%$

The measured efficiencies are listed in Table 7. We obtain an efficiency of $(99.7 \pm 0.1)\%$, $((99.7 \pm 0.1)\%$, $(99.7 \pm 0.1)\%$ for the ee ($e\mu$, $\mu\mu$) trigger with respect to the final di-lepton selection, respectively.

5 Efficiency for electrons and muons

The efficiency ratio is derived directly from the data but selection of an inclusive Z boson sample. For this we select di-lepton events (ee , $\mu\mu$) with (20,10) GeV including the lepton trigger paths listed in Sec.??.

We apply an cut in the invariant mass of $60 < m_{ll} < 120$ GeV to obtain a pure Z boson sample. The different flavour subtraction described in Sec. 7.1 relies on the knowledge of the electron to muon efficiency ratio, which we derive from this sample as

$$r_{\mu e} = \sqrt{\frac{n_{\mu\mu}}{n_{ee}}} = 1.13 \pm 0.07 \quad (3)$$

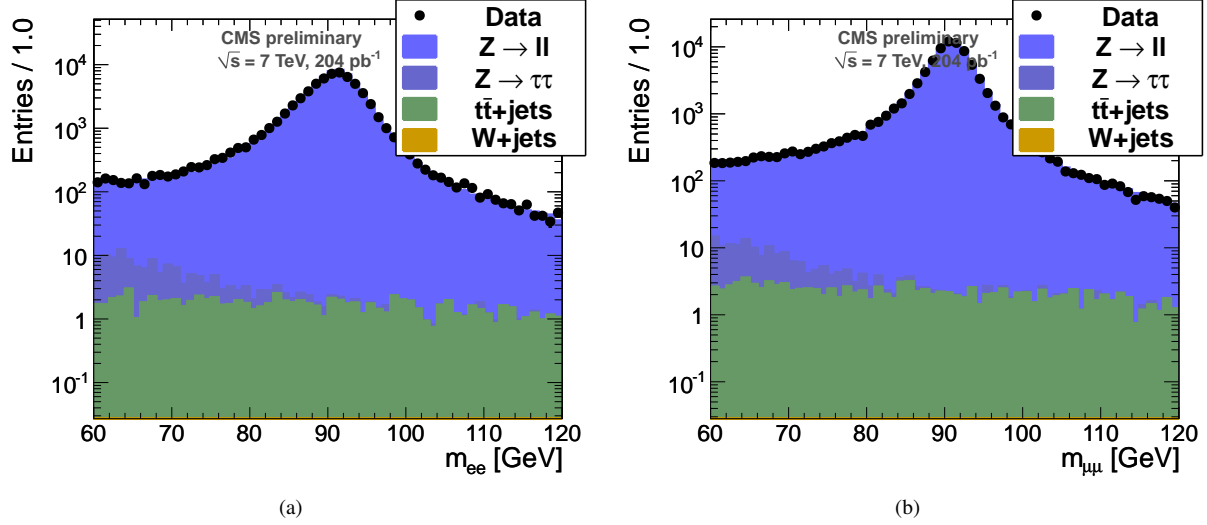


Figure 1: Invariant mass distributions for a (20,10) GeV di-lepton selection after leptonic trigger requirement.

Table 8: Muon to electron reconstruction efficiency ratio obtained from a Z boson selection on data and Z + jets Monte Carlo simulation.

	Data	Monte Carlo
ratio $r_{\mu e}$	$1.07 \pm 0.005(\text{stat}) \pm 0.05(\text{syst})$	$1.052 \pm 0.003(\text{stat})$

Since we measure the efficiency on a Z sample, which has a different jet multiplicity compared to a ttbar sample, we need to assign a systematic uncertainty in the extrapolation. We test the dependence in simulation by comparing a top MC sample with Z-boson simulation. While the absolute efficiency drops, the ratio of the electron to muon efficiency is approximately constant (within 5%), meaning that the loss in efficiency is the same for both lepton flavours. We therefore assume 5% additional systematic uncertainty on the ratio.

6 Event selection

For all event selections presented later on the main backgrounds are

Top pairs Top pair events are the dominant SM background to the search, since they contain real opposite sign leptons, missing transverse energy and a non negligible jet activity. This background is estimated by the opposite flavour subtraction.

Z+jets Events with a Z Boson contain two opposite sign leptons and can contain a high jet activity, but the missing transverse energy is always instrumental and therefore the background can be reduced completely. This background can be estimated using the JZB method [22] and is found to be very small in the signal region.

W+jets Events with a W Boson contain real missing transverse energy and can contain a high jet activity, but do only contain one lepton. Therefore the background can be measured using the fake lepton component. This background is estimated by the isolation template method.

Diboson Events with two gauge bosons do contribute to the background. Due to the low cross-section of the process their contribution is found to be negligible. This background is estimated from MC.

QCD Although the di-jet cross-section is huge, this background is found to be negligible in MC, since all cuts act very well on QCD (no isolated leptons, no missing transverse energy and a steeply falling H_T distribution). This background is estimated by the isolation template method.

6.1 Preselection

For now we select only events using the lepton trigger selection, but lower p_\perp leptons can be added without any changes to the presented methods. We start from a common preselection defined as

- Two leptons of opposite sign with the thresholds of $p_T > 20$ GeV for the hardest and $p_T > 10$ GeV for the second lepton.
- At least two jets and a $H_T > 100$ GeV.
- A missing transverse energy of at least $\cancel{E}_T > 100$ GeV.

The region is expected to be dominated by events with di-leptonic top decays. The yields in data and simulation are given in Tab. 9

Table 9: Summary of number of events expected from Monte Carlo simulations in the signal region of $H_T > 100$ GeV and $\cancel{E}_T > 100$ GeV. The errors reflect the Monte Carlo statistics only.

Process	ee	$\mu\mu$	$e\mu$	total
$t\bar{t}$	0.39 ± 0.04	0.5 ± 0.05	0.79 ± 0.06	1.68 ± 0.09
Z + jets	0.0 ± 0.07	0.08 ± 0.05	0.11 ± 0.07	0.19 ± 0.11
W + jets	0.0 ± 0.32	0.0 ± 0.32	0.0 ± 0.32	0.0 ± 0.32
Di-boson	0.02 ± 0.01	0.03 ± 0.01	0.03 ± 0.01	0.08 ± 0.02
Total background	0.41 ± 0.33	0.53 ± 0.33	$1. \pm 0.33$	$2. \pm 0.32$
Data	0	0	1	1
LM0	3.41 ± 0.17	3.91 ± 0.17	4.52 ± 0.14	11.84 ± 0.42
LM1	1.64 ± 0.04	2.02 ± 0.04	1.01 ± 0.03	4.64 ± 0.07

6.2 Definition of the signal regions

To be prepared for a much larger luminosity we define tighter signal regions for an integrated luminosity of up to 1 fb^{-1} .

6.2.1 2010 signal region

For reference we keep the signal region used in 2010. It is defined by tightening both H_T and \cancel{E}_T from the preselection region

- A $H_T > 350$ GeV.
- A $\cancel{E}_T > 150$ GeV.

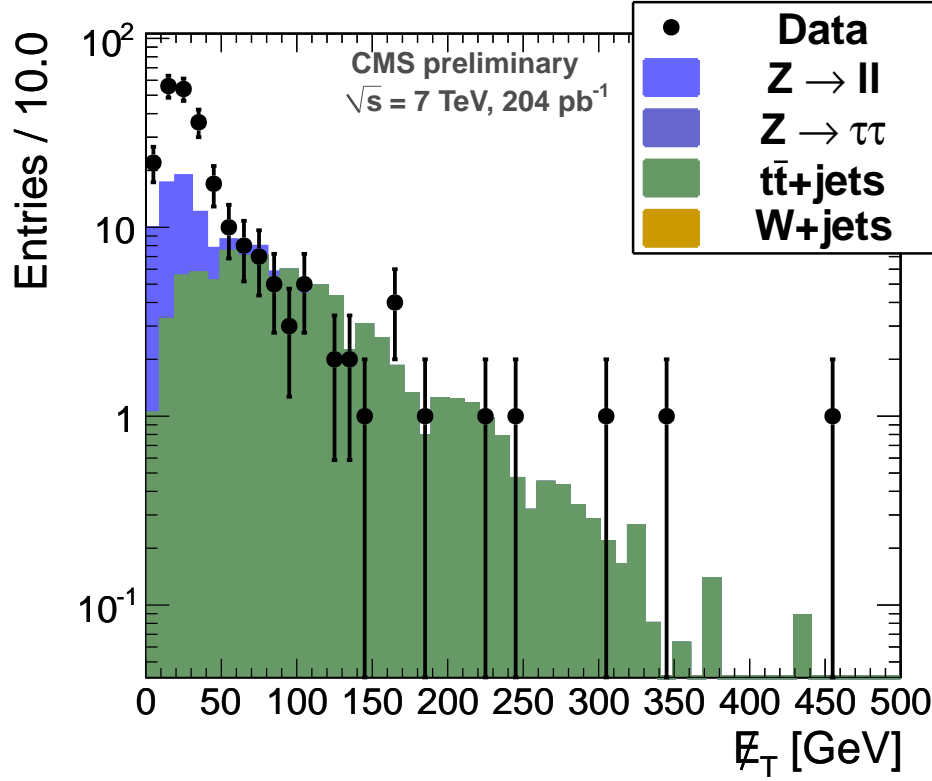
The \cancel{E}_T distribution after application of the H_T cut is shown in Fig 2(a) and the yield split by flavour for a cut at 150 GeV is listed in Tab. 10.

6.2.2 High H_T signal region

A signal region with high H_T is defined by tightening the H_T from the preselection region

- A $H_T > 600$ GeV.
- A $\cancel{E}_T > 100$ GeV.

The \cancel{E}_T distribution after application of the H_T cut is shown in Fig 4(a) and the yield split by flavour for a cut at 150 GeV is listed in Tab. 11.



(a)

Figure 2: \cancel{E}_T distribution for all events passing di-lepton selection and satisfy $H_T > 350$ GeV. For the final \cancel{E}_T selection (150) GeV the selection is dominated by $t\bar{t}$.

Table 10: Summary of number of events expected from Monte Carlo simulations in the signal region of $H_T > 350$ GeV and $\cancel{E}_T > 150$ GeV. The errors reflect the Monte Carlo (scaled to 204 pb⁻¹) statistics only.

Process	ee	$\mu\mu$	$e\mu$	total
$t\bar{t}$	0.39 ± 0.04	0.5 ± 0.05	0.79 ± 0.06	1.68 ± 0.09
$Z + \text{jets}$	0.0 ± 0.07	0.08 ± 0.05	0.11 ± 0.07	0.19 ± 0.11
$W + \text{jets}$	0.0 ± 0.32	0.0 ± 0.32	0.0 ± 0.32	0.0 ± 0.32
Di-boson	0.02 ± 0.01	0.03 ± 0.01	0.03 ± 0.01	0.08 ± 0.02
Total background	0.41 ± 0.33	0.53 ± 0.33	$1. \pm 0.33$	$2. \pm 0.32$
Data	0	0	1	1
LM0	3.41 ± 0.17	3.91 ± 0.17	4.52 ± 0.14	11.84 ± 0.42
LM1	1.64 ± 0.04	2.02 ± 0.04	1.01 ± 0.03	4.64 ± 0.07

6.2.3 High \cancel{E}_T signal region

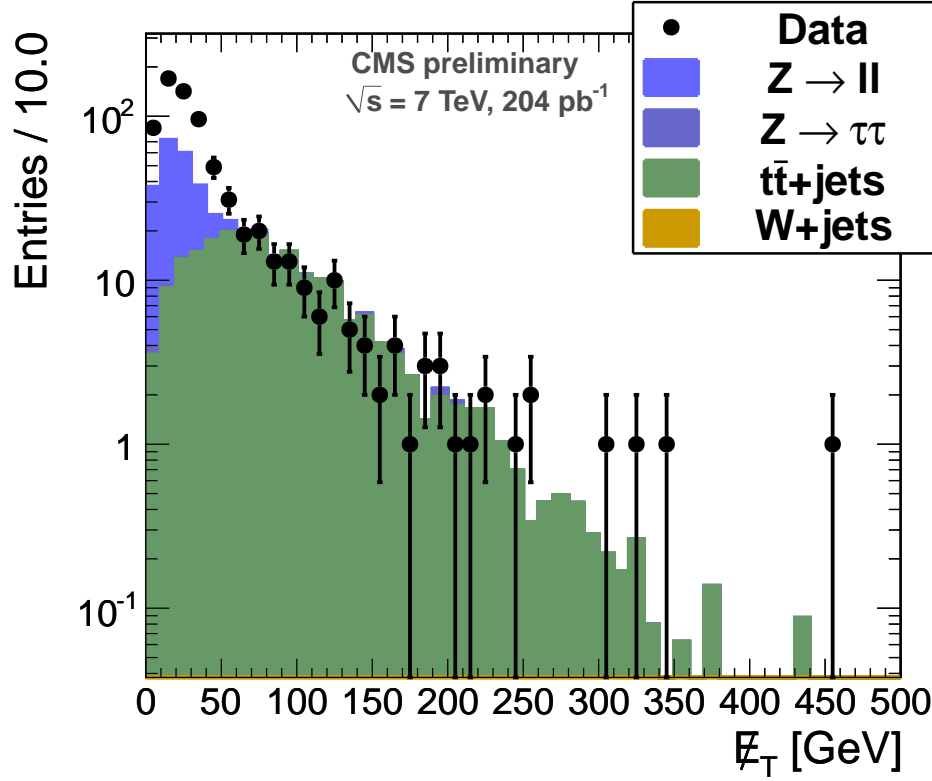
A signal region with high \cancel{E}_T is defined by slightly tightening the H_T and a much tighter \cancel{E}_T selection compared to the pre-selection region

- A $H_T > 250$ GeV.
- A $\cancel{E}_T > 250$ GeV.

The \cancel{E}_T distribution after application of the H_T cut is shown in Fig 4(a) and the yield split by flavour for a cut at 250 GeV is listed in Tab. 12.

7 Background prediction methods

We use three background prediction methods to estimate all backgrounds in the signal regions. Events where a fake or heavy flavour lepton fakes the signature of a di-lepton event (i.e. W+jets, Single Top, QCD) are estimated using



(a)

Figure 3: \cancel{E}_T distribution for all events passing di-lepton selection and satisfy $H_T > 600$ GeV. For the final \cancel{E}_T selection (100) GeV the selection is dominated by $t\bar{t}$.

Table 11: Summary of number of events expected from Monte Carlo simulations in the signal region of $H_T > 600$ GeV and $\cancel{E}_T > 100$ GeV. The errors reflect the Monte Carlo (scaled to 204 pb⁻¹) statistics only.

Process	ee	$\mu\mu$	$e\mu$	total
$t\bar{t}$	0.39 ± 0.04	0.5 ± 0.05	0.79 ± 0.06	1.68 ± 0.09
$Z + \text{jets}$	0.0 ± 0.07	0.08 ± 0.05	0.11 ± 0.07	0.19 ± 0.11
$W + \text{jets}$	0.0 ± 0.32	0.0 ± 0.32	0.0 ± 0.32	0.0 ± 0.32
Di-boson	0.02 ± 0.01	0.03 ± 0.01	0.03 ± 0.01	0.08 ± 0.02
Total background	0.41 ± 0.33	0.53 ± 0.33	$1. \pm 0.33$	$2. \pm 0.32$
Data	0	0	1	1
LM0	3.41 ± 0.17	3.91 ± 0.17	4.52 ± 0.14	11.84 ± 0.42
LM1	1.64 ± 0.04	2.02 ± 0.04	1.01 ± 0.03	4.64 ± 0.07

the fake rate method presented in Sec. ?? . Top pair, WW and $Z \rightarrow \tau\tau$ events are estimated from the $e\mu$ -control sample (Sec. 7.1). $Z \rightarrow ll$ ($l = e, \mu$) is estimated by extrapolating in H_T and \cancel{E}_T .

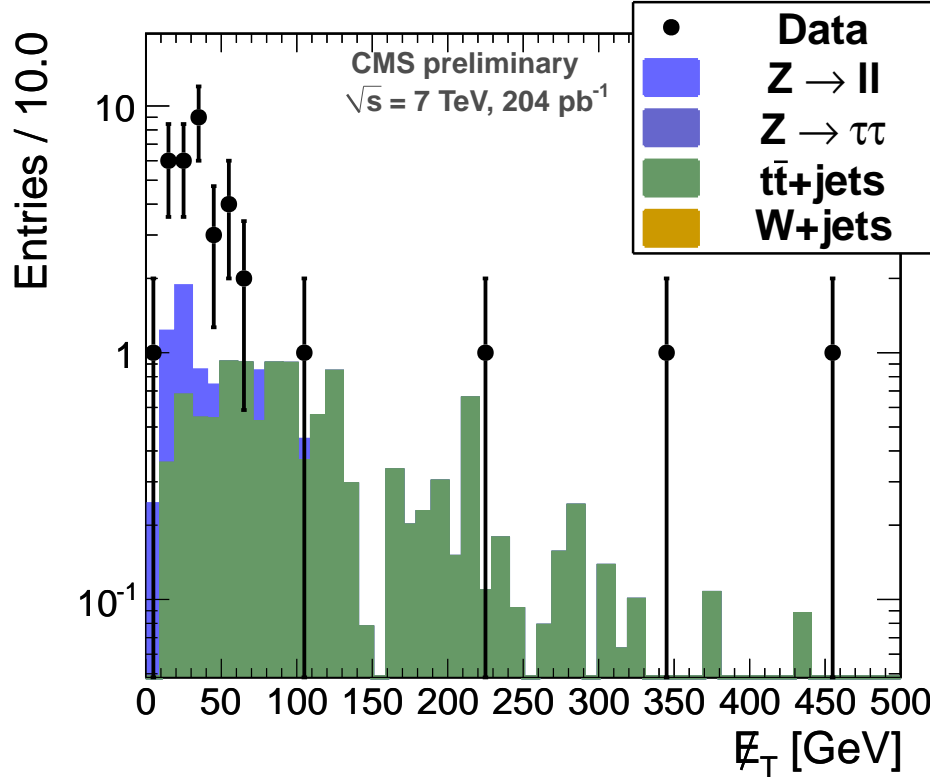
7.1 Different flavour subtraction

Since all signal regions are expected to be dominated by $t\bar{t}$ -production we use the different flavour control sample ($e\mu$) to predict backgrounds in which leptons uncorrelated in flavour are being produced. It relies only on the knowledge of the ratio of electron to muon reconstruction efficiency $r_{e\mu}$, which we derive in Sec. 5.

Under the assumption of lepton universality The following two formulas hold for any background where di-leptons are being produced uncorrelated (e.g. top-pairs events, $Z \rightarrow \tau^+\tau^- \rightarrow l^+l^-$, WW -production):

$$n_{ee} = \frac{1}{2} n_{e\mu} r_{\mu e}, \quad n_{\mu\mu} = \frac{1}{2} \frac{n_{e\mu}}{r_{\mu e}}.$$

A closure test of the method has been performed using a simulated top-pair sample (including pileup) and we



(a)

Figure 4: \cancel{E}_T distribution for all events passing di-lepton selection and satisfy $H_T > 250$ GeV. For the final \cancel{E}_T selection (250) GeV the selection is dominated by $t\bar{t}$.

Table 12: Summary of number of events expected from Monte Carlo simulations in the signal region of $H_T > 250$ GeV and $\cancel{E}_T > 250$ GeV. The errors reflect the Monte Carlo (scaled to 204 pb⁻¹) statistics only.

Process	ee	$\mu\mu$	$e\mu$	total
$t\bar{t}$	0.39 ± 0.04	0.5 ± 0.05	0.79 ± 0.06	1.68 ± 0.09
$Z + \text{jets}$	0.0 ± 0.07	0.08 ± 0.05	0.11 ± 0.07	0.19 ± 0.11
$W + \text{jets}$	0.0 ± 0.32	0.0 ± 0.32	0.0 ± 0.32	0.0 ± 0.32
Di-boson	0.02 ± 0.01	0.03 ± 0.01	0.03 ± 0.01	0.08 ± 0.02
Total background	0.41 ± 0.33	0.53 ± 0.33	$1. \pm 0.33$	$2. \pm 0.32$
Data	0	0	1	1
LM0	3.41 ± 0.17	3.91 ± 0.17	4.52 ± 0.14	11.84 ± 0.42
LM1	1.64 ± 0.04	2.02 ± 0.04	1.01 ± 0.03	4.64 ± 0.07

observe a good agreement between prediction and MC truth:

$$n_{ee} = ?? .9 \pm 2.8(\text{stat.}) \text{ } (?? .2 \text{ MC}), \quad n_{\mu\mu} = ?? .8 \pm 3.3(\text{stat.}) \text{ } (?? .5 \text{ MC}).$$

Later in this note we are only interested in an excess of $ee + \mu\mu$ and in this extrapolation the ratio largely cancels as long as the differences in lepton efficiencies are not large.

7.2 Z boson prediction

Backgrounds containing a real di-lepton pair of same flavour (ee and $\mu\mu$) are estimated by a partly data-driven extrapolation in H_T and \cancel{E}_T . We start by extraction of the Z yield using a fit to the invariant mass distribution in the preselection region ($H_T > 100$ GeV and $\cancel{E}_T > 100$ GeV). From the fit we extract a yield of

$$n_{Z,\text{control}} = 5.4 \pm 3.4_{\text{stat}} \quad (4)$$

in $ee + \mu\mu$ modes. This yield is used to derive a prediction in the signal regions

$$n_{Z,sig} = \epsilon_{H_T} \epsilon_{\cancel{E}_T} n_{Z,control}, \quad (5)$$

where ϵ_{H_T} and $\epsilon_{\cancel{E}_T}$ describe an extrapolation in H_T and \cancel{E}_T respectively.

The extrapolation in H_T is performed fully data-driven by fitting the Z yield without \cancel{E}_T cut. For this we select events for $H_T \lesssim 100$ GeV, $H_T \lesssim 250$ GeV, $H_T \lesssim 350$ GeV and $H_T \lesssim 600$ GeV, which correspond to the H_T thresholds used in various signal regions. By using the ratio of the yields in these regions we drive the efficiency of the H_T cut

$$\epsilon_{H_T} = \frac{n_{Z,H_T,signal}}{n_{Z,H_T,control}}. \quad (6)$$

The yields and efficiencies for all regions are summarised in Tab. ??.

Table 13: Z yield in.

H_T thresh. [GeV]	Yield n_Z	ϵ_{H_T}
100	3191 \pm ??	1.
250	158 \pm ??	??. 8 ± 0.1
350	51 \pm ??	??. 8 ± 0.1
600	21 \pm ??	?? ± 0.1

The extrapolation in \cancel{E}_T is performed from simulation after applying the \cancel{E}_T and H_T cut of the preselection. We find that suppression in \cancel{E}_T is reduced after application of a higher H_T selection, but the simulation is statistically limited in this region. The systematic uncertainty on this extrapolation is assumed to be 50%.

We derive a extrapolation factor of

$$\epsilon_{\cancel{E}_T, 100 \rightarrow 150} = 0.5 \pm 0.25 \quad (7)$$

for a H_T threshold of 250 GeV and 350 GeV. For higher \cancel{E}_T selections no events are selected according to simulation, thus we derive an upper limit on the number of events in that region.

For all signal regions the expected Z yield is rather low, so that a large systematic uncertainty can be accommodated.

7.3 Preselection region

In the pre-selection region ($H_T \lesssim 100$ GeV and $\cancel{E}_T \lesssim 100$ GeV) we perform a full shape analysis of the different ($e\mu$) an same flavour (ee , $\mu\mu$) lepton pairs.

A data to MC comparison of all same flavour events is shown in Fig. 5(a) for all same flavour and in Fig. 5(b) for the different flavour pairs. It is seen that data and simulation do agree relatively good.

In this region we perform a full shape analysis of the same and different flavour lepton pairs. The fit of the $e\mu$ lepton pairs is shown in Fig. 6(b). This background is described by

$$B(m_{ll}) = m_{ll}^a \cdot e^{-b \cdot m_{ll}}. \quad (8)$$

The green band represents the statistical uncertainty on the shape.

The same flavour lepton pairs are fitted by the background shape from $e\mu$ with the normalisation fixed within the statistical plus systematical uncertainty from the $e\mu$ -pairs.

For a potential signal the an edge model is fitted and the Z contribution is modelled by a Breit-Wigner convoluted with a Gaussian.

The fit of the $ee + \mu\mu$ lepton pairs is shown in Fig. 6(a).

It is seen that no significant contribution above the background is observed.

8 Results

In Tab. 14 the yields and the background predictions from the three methods are listed for the signal region used for the analysis of the 2010 data. Good agreement between prediction and observation is seen.

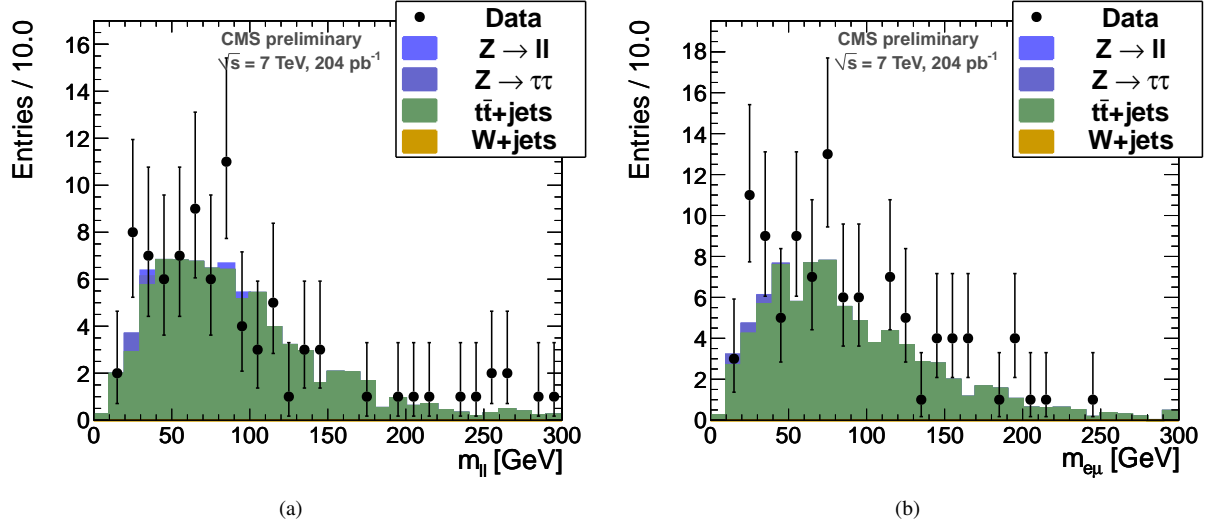


Figure 5: Data to MC comparison for events in the pre-selection region ($HT > 100 \text{ GeV}$, $\cancel{E}_T > 100 \text{ GeV}$) for an integrated luminosity of 204 pb^{-1} . (a) shows the $ee + \mu\mu$ -pairs and (b) $e\mu$ -pairs.

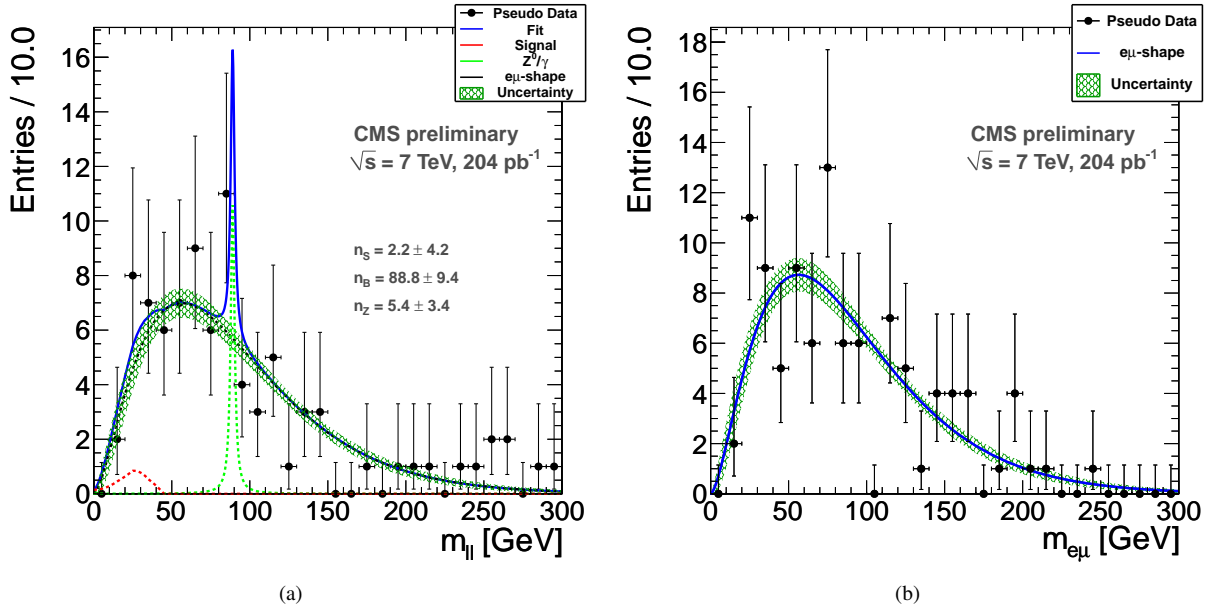


Figure 6: Data to MC comparison for events in the pre-selection region ($HT > 100 \text{ GeV}$, $\cancel{E}_T > 100 \text{ GeV}$) for an integrated luminosity of 204 pb^{-1} . (a) shows the $ee + \mu\mu$ -pairs and (b) $e\mu$ -pairs.

Table 14: Number of predicted and observed events in the 2010 signal region, defined as: $H_T > 350$ GeV and $\vec{E}_T > 150$ GeV.

	2010 signal region	
Process	ee	$\mu\mu$
tt from $e\mu$	11.7 ± 2.4	13.4 ± 2.8
Fake leptons	0.5 ± 0.3	0.4 ± 0.2
Total predicted	12.2 ± 2.4	13.8 ± 2.8
Total observed	10	15
SM MC	8.4 ± 0.2	10.5 ± 0.3
LM0	3.7 ± 0.2	4.2 ± 0.2
LM1	0.5 ± 0.1	0.7 ± 0.1

In Tab. 16 the yields and the background predictions from the three methods are listed for the signal region defined by a tight \vec{E}_T selection. We observe good agreement between prediction and observation.

Table 15: Number of predicted and observed events in the high \vec{E}_T signal region, defined as: $H_T > 250$ GeV and $\vec{E}_T > 250$ GeV.

	High \vec{E}_T Region	
Process	ee	$\mu\mu$
tt from $e\mu$	11.7 ± 2.4	13.4 ± 2.8
Fake leptons	0.5 ± 0.3	0.4 ± 0.2
Total predicted	12.2 ± 2.4	13.8 ± 2.8
Total observed	10	15
SM MC	8.4 ± 0.2	10.5 ± 0.3
LM0	3.7 ± 0.2	4.2 ± 0.2
LM1	0.5 ± 0.1	0.7 ± 0.1

Tab. 16 compares the yields and the background predictions from the three background prediction methods for the signal region defined by a tight H_T selection. A good agreement between prediction and observation can be seen.

Table 16: Number of predicted and observed events in the high H_T signal region, defined as: $H_T > 600$ GeV and $\vec{E}_T > 100$ GeV.

	High H_T region	
Process	ee	$\mu\mu$
tt from $e\mu$	11.7 ± 2.4	13.4 ± 2.8
Fake leptons	0.5 ± 0.3	0.4 ± 0.2
Total predicted	12.2 ± 2.4	13.8 ± 2.8
Total observed	10	15
SM MC	8.4 ± 0.2	10.5 ± 0.3
LM0	3.7 ± 0.2	4.2 ± 0.2
LM1	0.5 ± 0.1	0.7 ± 0.1

We find one event in the signal region in the $e\mu$ -lepton combination with a fake prediction of 0.1 ± 0.1 , and thus predict $0.9^{+2.2}_{-0.8}$ same-flavour events. In data we find no same-flavour events and have to contrast this with 7.3 ± 1.6 and (3.6 ± 0.7) expected events at the benchmark points LM0 (LM1).

9 Limit

As discussed in Section 8, we see no event in the signal region, defined as $H_T > 350$ GeV and $\vec{E}_T > 150$ GeV and two same flavour opposite sign leptons.

The background prediction from the SM Monte Carlo is 0.77 ± 0.26 events, where the uncertainty comes from the jet energy scale (30%, see Section ??), the luminosity (11%), and the lepton/trigger efficiency (10%)²⁾. The opposite flavor based background prediction is $0.9^{+2.2}_{-0.8}$.

The background prediction is well in agreement with the prediction from simulation and with the observation of no events.

We calculate a Bayesian 95% CL upper limit [26] on the number of non SM events in this signal region to be 3.0.

We cross-checked the code with a Bayesian 95% CL upper limit using the MCMC calculator[27] and get the same result of 3.0.

Here as well, we remind the reader of the number of expected LM0 and LM1 events from Table ?? : 7.3 ± 1.6 events and 3.3 ± 0.7 respectively, where the uncertainties are from energy scale (Section ??), luminosity, and lepton efficiency.

We thus can exclude LM0 95% confidence level.

10 Conclusion

We have presented a SUSY search for correlated flavour production in the opposite-sign channel in the presence of high H_T and \cancel{E}_T . We observe good agreement between data and simulation as well as to our background prediction method. We conclude that there is no sign of flavour correlated production and set a limit 3.0 signal events at 95% confidence level within acceptance of our selection. This excludes the discussed benchmark points LM0.

11 Acknowledgements

References

- [1] B.C. Allanach, "SOFTSUSY: a program for calculating supersymmetric spectra", Comput.Phys.Commun. 143:305-331, 2002
- [2] A. Djouadi et al, *Decays of Supersymmetric Particles: the program SUSY-HIT (SUspect-SdecaY-Hdecay-InTerface)* ActaPhys.Polon. B38:635-644, 2007.
- [3] T. Sjostrand et al, "PYTHIA 6.4 Physics and Manual", JHEP 0605:026, 2006
- [4] W. Beenakker et al, "Squark and Gluino Production at Hadron Colliders", Nucl.Phys. B492:51-103, 1997
- [5] The CMS Collaboration, "Study of the Z production in association with jets in proton-proton collisions at $\sqrt{s} = 10$ TeV with the CMS detector at the CERN LHC", CMS Physics Analysis Summary JME-08-006
- [6] M. Cacciari et al, "The anti- k_t jet clustering algorithm", JHEP 0804:063, 2008
- [7] J. Alwall et al, "MadGraph/MadEvent v4: The New Web Generation", JHEP 0709:028, 2007
- [8] M. Cacciari et al, "Updated predictions for the total production cross sections of top and of heavier quark pairs at the Tevatron and at the LHC", JHEP 0809:127, 2008
- [9] S. Frixione, M.L. Mangano, "How accurately can we measure the W cross section?", JHEP 0405:056, 2004
- [10] M. Pivk and F.R. Le Diberder, *A statistical tool to unfold data distributions*, arXiv:physics/0402083
- [11] V+jets wiki, <https://twiki.cern.ch/twiki/bin/view/CMS/VplusJets>
- [12] M. Mulders et al. "Muon Identification in CMS", CMS Analysis Note 2008/098
- [13] J. Branson et al. "A cut based method for electron identification in CMS", CMS Analysis Note 2008/082
- [14] F. Beaudette et al. "Electron Reconstruction within the Particle Flow Algorithm", CMS Analysis Note 2010/034
- [15] M. Bachtis et al. "Commissioning of the Particle-flow Event Reconstruction with the first LHC collisions recorded in the CMS detector", CMS Analysis Note 2010/???

²⁾ Other uncertainties associated with the modeling of $t\bar{t}$ in MadGraph have not been evaluated.

- 362 [16] G. P. Salam, G. Soyez, "A practical Seedless Infrared-Safe Cone jet algorithm", JHEP 0705:086, 2007
- 363 [17] The CMS Collaboration, "Plans for Jet Energy Corrections at CMS", CMS Physics Analysis Summary
364 JME-07-002
- 365 [18] N. Saoulidou, "Particle Flow Jet Identification Criteria", CMS Analysis Note 2009/???
- 366 [19] W. Verkerke, D. Kirkby, "The RooFit toolkit for data modeling", arXiv:physics/0306116
- 367 [20] The CMS Collaboration, "Performance of muon identification in pp collisions at $\sqrt{s} = 7 \text{ TeV}$ ", CMS Physics
368 Analysis Summary MUO-10-002
- 369 [21] The CMS Collaboration, "Performance of Methods for Data-Driven Background Estimation in SUSY
370 Searches", CMS Physics Analysis Summary SUS-10-001
- 371 [22] K. Theofilatos et al. "SUSY Searches in the $Z^0 + 3 \text{ jets} + \cancel{E}_T$ Final State with Data-driven Background
372 Estimation", CMS Analysis Note 2009/132
- 373 [23] A. Singh et al. "SUSY in the $Z/\gamma^* + \text{Jet}(s) + \cancel{E}_T$ Final State Using Particle Flow", CMS Analysis Note
374 2010/250
- 375 [24] B. Hooberman et al. "Search for new physics in the opposite sign dilepton sample", CMS Analysis Note
376 2010/370
- 377 [25] J. Conway, <https://twiki.cern.ch/twiki/bin/view/CMS/PileupInformation>
- 378 [26] J. Conway, <http://www-cdf.fnal.gov/physics/statistics/code/bayes.f>
- 379 [27] RooStats wiki, <https://twiki.cern.ch/twiki/bin/view/RooStats/WebHome>
- 380 [28] The CMS Collaboration, "Measurement of CMS Luminosity", CMS Physics Analysis Summary EWK-10-
381 004
- 382 [29] The CMS Collaboration, "Jet Energy Corrections determination at $\sqrt{s} = 7 \text{ TeV}$ ", CMS Physics Analysis
383 Summary JME-10-010
- 384 [30] The CMS Collaboration, "MET Performance in Events Containing Electroweak Bosons from pp Collisions
385 at $\sqrt{s} = 7 \text{ TeV}$ ", CMS Physics Analysis Summary JME-10-005